Low Temperature Plasma Technology Laboratory

CENTRAL PEAKING OF

MAGNETIZED GAS DISCHARGES

Francis F. Chen and Davide Curreli

LTP-1210   Oct. 2012

LTPTL

Electrical Engineering Department
Los Angeles, California 90095-1594

UNIVERSITY OF CALIFORNIA • LOS ANGELES

Central peaking of magnetized gas discharges

Francis F. Chen[*]**,** *Electrical Engineering Department, University of California, Los Angeles, California 90095* and

Davide Curreli[†]**,** *Department of Nuclear, Plasma and Radiological Engineering, University of Illinois at Urbana Champaign*

ABSTRACT

Partially ionized gas discharges used in industry are often driven by radiofrequency (rf) power applied at the periphery of a cylinder. It is found that the plasma density n is usually flat or peaked on axis even if the skin depth of the rf field is thin compared with the chamber radius a. Previous attempts at explaining this did not account for the finite length of the discharge and the boundary conditions at the endplates. A simple 1D model is used to focus on the basic mechanism: the short-circuit effect. It is found that a strong electric field (E-field) scaled to electron temperature T_e, drives the ions inward. The resulting density profile is peaked on axis and has a shape independent of pressure or discharge radius. This "universal" profile is not affected by a dc magnetic field (B-field) as long as the ion Larmor radius is larger than a.

I. Introduction

The motivation for this work was the observation that $n(r)$ is peaked on axis in both magnetized (helicon) and unmagnetized (ICP, Inductively Coupled Plasma) discharges even though the rf power is applied to a thin layer at the cylindrical periphery. In ICPs, the rf skin depth is typically 3 cm, much shorter than a typical a of 10 cm. In helicons, most of the rf power is absorbed by excitation of the Trivelpiece-Gould (TG) mode in a layer of typical thickness ≤5mm, and yet n almost never has a hollow profile. Most theory on gas discharges do not tackle the problem of equilibrium profiles; rather, they are about distribution functions and collision cross sections, which are peripheral to the problem of central peaking though they may have small effects on the details. This paper is a short version of our complete paper[1], published earlier, which contains the appropriate references

A previous attempt[2] had been made to solve this problem. The orbit of an electron in a cylinder with rf applied only at the circumference was traced through many rf cycles with the nonlinear radial Lorentz force $\mathbf{F}_L = -e\tilde{\mathbf{v}} \times \tilde{\mathbf{B}}$ included. It was found that indeed the density was peaked on axis, partly because electron orbits crossed there, and partly because electrons were slow when they reached the center. However, this was in the usual theoretical infinite cylinder.

Our approach here is to strip the problem of all unnecessary details, taking a cylindrical discharge tube and neglecting azimuthal variations. The usual infinite cylinder would not be realistic, so we assume a tube length that is short enough that we can neglect variations in the axial direction z, but long enough that ions can cross the B-field by collisions. A tube of such intermediate aspect ratio is shown in Fig. 1

---

[*] ffchen@ee.ucla.edu
[†] dcurreli@illinois.edu

When there is a *B*-field, the electrons will be confined to move mainly along the field lines, but we shall see that this is not a necessary assumption. We do assume that the *B*-field is weak enough that the ion Larmor radius is much larger than *a*. The ion orbits will be curved, but this curvature can be neglected if we assume azimuthal symmetry and reduce to a one-dimensional problem in radius *r*.

Now, there is a problem of boundary conditions. The radial boundary has to be non-conducting, since the antenna is located outside. The endplates can be metal or dielectric; it will not matter. The electrons will travel rapidly to the endplates, and a sheath will form to prevent them from leaving the discharge faster than the ions, thus preserving quasineutrality. The sheath thickness and potential drop ("sheath drop") can vary with *r*. This variation causes a phenomenon called the "short-circuit effect"[3], which requires explanation.
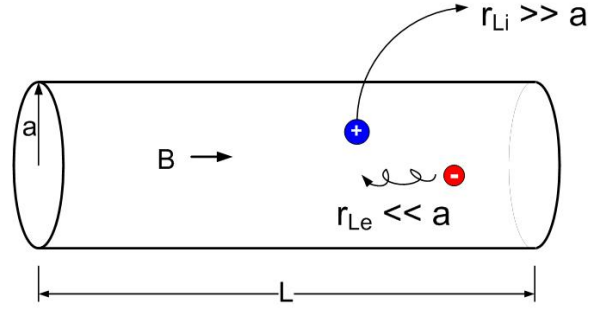

Fig. 1. An assumed discharge geometry.

II. The short-circuit effect

Figure 2a shows the sheath conditions at one endplate. Assume that ionization occurs more strongly near the radial boundary, so that *n* is higher in magnetic tube (1) than in tube (2), which is closer to the axis. Assume a strong *B*-field so that electrons move only along **B**, bouncing between the end-plate sheaths. Electrons in each small tube will fall into a Maxwellian distribution with a temperature T_e; but there is no communication between tubes, so T_e can be different in each tube. The ion flux to the endplate will be nc_s, since ions will enter the sheath with the Bohm velocity, which is equal to the acoustic speed c_s. For equal ion and electron fluxes, the sheath drop must satisfy

$$n\left(\frac{KT_e}{2\pi m}\right)^{\!\frac{1}{2}} e^{-e\phi_p/KT_e} = n\left(\frac{KT_e}{M}\right)^{\!\frac{1}{2}}, \qquad \frac{e\phi_p}{KT_e} = \ln\left(\frac{M}{2\pi m}\right)^{\!1/2}, \tag{1}$$

where φ_p is the (positive) plasma potential relative to the endplate, and the brackets are the electron thermal speed on the left and c_s on the right. The sheath drop φ_p is independent of density, and normally would be the same in tubes (1) and (2). However, as the ions drift from (1) to (2) due to the density gradient, the density in (2) is increased, and the sheath drop there must increase, trapping more electrons to keep the plasma neutral. Thus, electrons *seem* to have moved with the diffusing ions, but their density was adjusted only by a small adjustment of their losses through the sheath. This short-circuit mechanism takes only a few nanoseconds, the time for electrons to move along **B**. Once the electrons are able to "move" across **B**, they will fall into a thermal distribution following the Boltzmann relation:
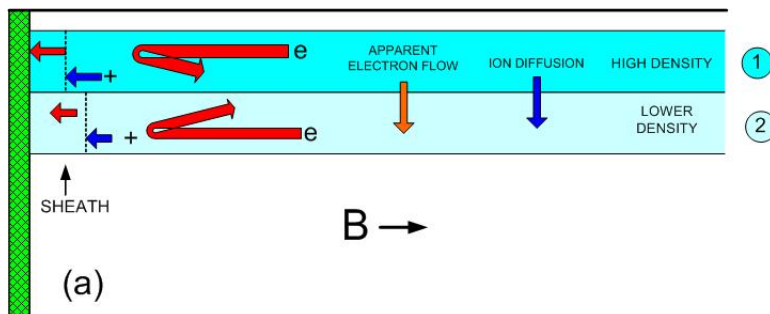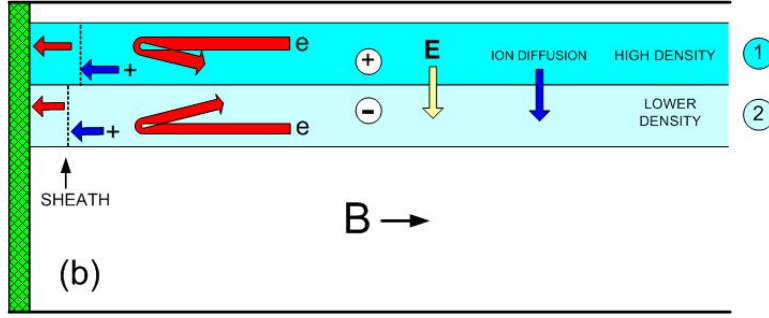
Fig. 2. Illustration of the short-circuit effect. Magnetic tube (1) has higher density than tube (2). The sheath thickness has been greatly exaggerated. (a) During short-circuiting; (b) During approach to equilibrium.

$$n = n_0 e^{e\phi/KT_e} \equiv n_0 e^{-\eta} . \tag{2}$$

Here KT_e can vary with r, since the short circuit effect does not actually move electrons across $\mathbf{B}$, and each magnetic tube can retain its original T_e. With Eq. (2) satisfied everywhere, φ is high were n is high, and we have the situation in Fig. 2b. There is now a radial electric field E_r, scaled to T_e, driving the ions inward much faster than diffusion at temperature T_i. When the ions begin to pile up at the center, ϕ is high there, and the E-field reverses to drive the ions outward. In equilibrium, both n and ϕ peak on axis, and the outward E-field accelerates ions up to the Bohm velocity at the sheath edge.

III. The ion equation

The steady-state ion motion can be described sufficiently well by the cold-fluid equation[4].

$$M\mathbf{v}\nabla \cdot (n\mathbf{v}) + Mn\mathbf{v} \cdot \nabla\mathbf{v} - en\mathbf{E} + Mn\nu_{io}\mathbf{v} = en(\mathbf{v}\times\mathbf{B}) - KT_i\nabla n \approx 0 . \tag{3}$$

Here M is the ion mass, $\mathbf{v}$ the ion fluid velocity, and ν_{io} the charge-exchange collision frequency. The first term in Eq. (3) accounts for drag due to ionization, which injects slow ions into the fluid. The two terms on the right-hand side will be neglected, the $\mathbf{v}\times\mathbf{B}$ term because we are neglecting ion curvature, and the T_i term because T_i is usually $<<T_e$. The ions will be accelerated by $\mathbf{E}$, which scales with T_e. The ion equation of continuity is

$$\nabla \cdot (n\mathbf{v}) = nn_n P_i(r) , \tag{4}$$

where n_n is the density of neutrals, and P_i is the ionization probability. P_i and the collision probability are defined by

$$P_i(r) \equiv <\sigma v>_{ion}(r), \quad P_c(r) \equiv <\sigma v>_{cx}(r) = \nu_{io}/n_n . \tag{5}$$

Using Eqs. (4) and (5) in Eq. (3) yields

$$M\mathbf{v}\cdot\nabla\mathbf{v} - e\mathbf{E} + Mn_n(P_i + P_c)\mathbf{v} = 0 . \tag{6}$$

With the usual definitions

$$\mathbf{E} = -\nabla\phi, \quad \eta \equiv -e\phi/KT_e, \quad \text{and} \quad c_s \equiv (KT_e/M)^{1/2}, \tag{7}$$

the radial component of Eq. (6) becomes

$$v \frac{dv}{dr} = c_s^2 \frac{d\eta}{dr} - n_n (P_c + P_i) v, \tag{8}$$

and the radial component of Eq. (4) is

$$\frac{dv}{dr} + v \frac{d(\ln n)}{dr} + \frac{v}{r} = n_n P_i(r). \tag{9}$$

The derivative of Eq. (2) can be written

$$\frac{d(\ln n)}{dr} = -\frac{d\eta}{dr}. \tag{10}$$

With this, Eq. (9) simplifies to

$$\frac{dv}{dr} - v \frac{d\eta}{dr} + \frac{v}{r} = n_n P_i(r). \tag{11}$$

The factor $d\eta/dr$ can be eliminated by using Eq. (8), resulting in a simple first-order differential equation for the ion velocity v:

$$\frac{dv}{dr} + \frac{v}{r} - \frac{v^2}{c_s^2} \left[\frac{dv}{dr} + n_n (P_i + P_c) \right] = n_n P_i(r), \quad \text{or} \tag{12}$$

$$\frac{dv}{dr} = \frac{c_s^2}{c_s^2 - v^2} \left[-\frac{v}{r} + n_n P_i(r) + \frac{v^2}{c_s^2} n_n (P_i + P_c) \right]. \tag{13}$$

This equation has the desirable property that dv/dr approaches infinity as v reaches c_s (the Bohm criterion), making a natural transition to the much thinner Debye sheath. Solutions of this equation yields the equilibrium profile of v, from which the desired profiles of n and ϕ can be calculated.

IV. Properties of the equilibrium profile

All quantities in Eq. (13) can be functions of r which can be calculated with refinements outside the scope of this paper. For instance, a neutral-depletion calculation yields $n_n(r)$. The weak dependence of charge-exchange probability P_c on v can be included easily. However, $T_e(r)$ depends on energy deposition of the particular discharge type, and we much assume T_e to be constant here. The ionization probability P_i varies exponentially with T_e, so our results will be sensitive to the assumed T_e. The properties of Eq. (13) are more easily seen if we introduce dimensionless variables:

$$u \equiv v/c_s, \qquad k(r) \equiv 1 + P_c(r)/P_i(r). \tag{14}$$

Eq. (13) becomes

$$\frac{du}{dr} = \frac{1}{1 - u^2} \left[-\frac{u}{r} + \frac{n_n}{c_s} P_i (1 + ku^2) \right]. \tag{15}$$

We next rescale r to remove n_n from this equation, defining

$$\rho \equiv (n_n P_i / c_s) r, \tag{16}$$

which yields

$$\frac{du}{d\rho} = \frac{1}{1-u^2}\left[1 + ku^2 - \frac{u}{\rho}\right].$$ (17)

The variable ρ contains some of the discharge parameters, and those that are left—namely, P_c/P_i — are in the parameter k in the nonlinear term. Note that the magnetic field **B** is irrelevant.

V. Solutions for constant n_n and T_e

If n_n and T_e are fixed, k is also constant. Figure 3 shows solutions of Eq. (17) for three values of k. Each value gives a curve that reaches $v/c_s = 1$ at a different radius ρ, called ρ_a. Neglecting the sheath thickness, we can identify ρ_a with the discharge radius a. When we rescale ρ for each curve so that their ρ_a's are the same, we find that the curves are self-similar and all become the same curve. This is the curve v/c_s in Fig. 4, plotted against r/a together with the corresponding profiles of n and ϕ. We thus have a "universal" equilibrium profile independent of neutral density n_n. It is also independent of the size of the plasma. A plot similar to Fig. 4 appears as Fig. 12 in Ref. (5).
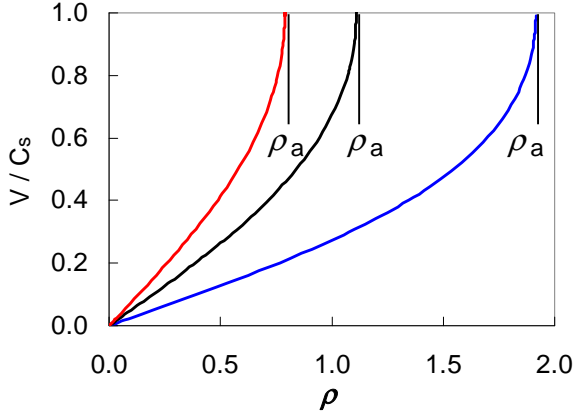

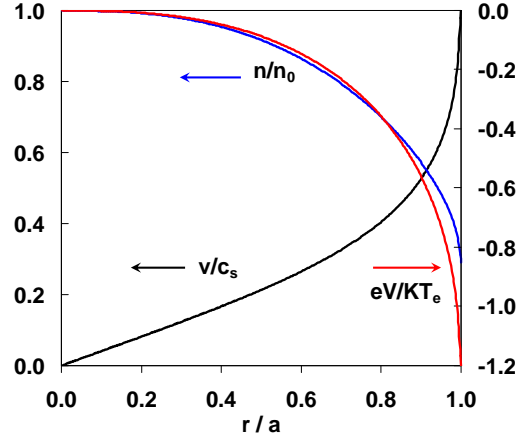Fig. 3. Solutions of Eq. (17) for three different values of k.

Fig. 4. Rescaled solution of Eq. (17) for 15 mTorr of argon and $KT_e = 3$ eV.

Since P_i varies strongly with T_e, this "universal" $n(r)$ profile *does* change when T_e is changed. This is shown in Fig. 5.
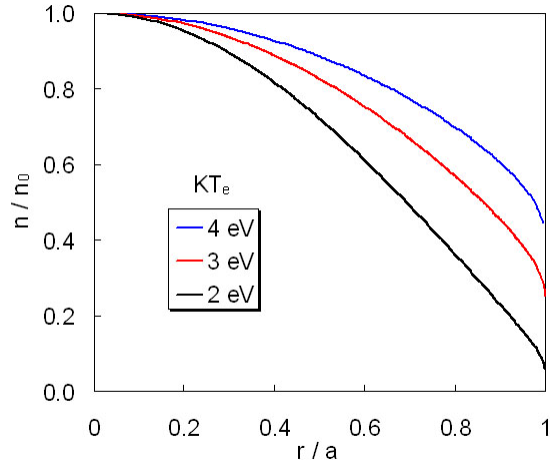
Fig. 5. Equilibrium $n(r)$ profiles at various electron temperatures. The curves are in the same order as the legend (color online).

The situation is not quite so simple because of ionization balance, which requires that the net loss of ions from each cylindrical shell δr be equal to the input from ionization. The necessary equation is

$$\frac{1}{nr}\frac{d}{dr}(rnv) = n_n P_i(T_e).$$
(18)

This has to be solved simultaneously with the *dimensional* equation (13). The result is that T_e is not arbitrary but depends on the plasma size a. As seen in Fig. 6, only one T_e gives a $v(r)$ profile that fits into a 5-cm diam tube.
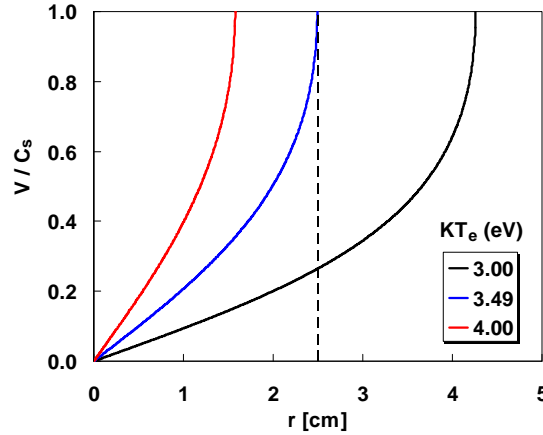

Fig. 6. Profiles of $v(r)$ in a 2.5-cm radius, 10-mTorr argon discharge.

When neutral depletion is included, there are three differential equations, including Eqs. (13) and (18), to be be solved simultaneously. One of us (DC) has written a code EQM which does this and yields equilibrium profiles for all discharges with aspect ratios fitting our original assumptions. The examples given above are for uniform T_e, but EQM handles arbitrary $T_e(r)$. This code is then coupled to the HELIC code[6] to give exact results for helicon discharges, including the value of $T_e(r)$. Details are given in Ref. 1.

VI. Discussion

By reducing the problem of equilibrium radial profiles of partially ionized gases to its basic elements, we have found that these profiles tend to have a universal shape regardless of the neutral pressure and discharge radius. The key novel feature is the short-circuit effect at the endplates, which allows electrons to cross the B-field in a practical sense, though not actually. The electrons then follow the Boltzmann relation, resulting in an E-field that initially drives the ions inward even if they are created at the edge, and later drives the ions outward after a centrally peaked density profile has been set up. It is found that the equilibrium profiles have an almost universal shape, independent of pressure and B-field. The results apply to all discharges, magnetized or not, of the type shown in Fig. 1.

The physical reason for centrally peaked profiles derives from the fact that sheath adjustments at the endplates allow electrons to effectively move across $\mathbf{B}$. This allows electrons to follow the Boltzmann relation, even across $\mathbf{B}$. In that case, $n(r)$ must peak on axis in order for $\phi(r)$ to peak there. If $\phi(r)$ did not peak there, the associated E-field would drive ions inwards,

where they would have nowhere to go, since diffusion along **B** at the ion temperature is very slow. There are situations where our assumptions are not valid and $n(r)$ is not peaked on axis, and we have observed these[7].

In Fig. 4 the density profile is seen to be independent of pressure, although the pressure does appear in the definition of ρ. The physical reason for this is that v is required to reach c_s at $r = a$, and the E-field provides a feedback mechanism. If, for instance, $n(r)$ is too steep at one r, the E-field there would be stronger than normal, and the ions would be accelerated to smooth out the $n(r)$ profile. This adjustment has to be made regardless of the pressure.

Although the short-circuit effect maintains overall neutrality of the plasma in the interior of the discharge, a problem arises with losses to the radial wall. Since the ions are unmagnetized, they have the same flux radially as they have axially; but electrons cannot move radially to balance these large radial ion losses. If the radial wall is a grounded conductor, an escaping ion can be neutralized by an electron from the wall and be re-injected as a neutral atom. However, if the wall is insulating, the ions will charge it positively; and a magnetic sheath will build up to slow down their escape. The radial ion flux has to be balanced by a radial electron flux, which can be generated only by cross-field diffusion of electrons via electron-ion and electron-neutral collisions. Thus, there will be layer about an electron Larmor diameter thick in which the radial electron flux is generated. In this layer ions and electrons are lost both axially and radially. The sheath fields will modify the shape of the electron gyro-orbits. The radial sheath cannot be treated with the fluid theory used in this paper is therefore outside the purview of this paper. Since we assumed small electron Larmor radii, this layer will be thin enough to be neglected in the equilibrium profiles calculated here.

VII. Acknowledgments

REFERENCES

[1] D. Curreli and F.F. Chen, Phys. Plasmas **18**, 113501 (2011).

[2] F.F. Chen, IEEE Trans. Plasma Sci. **34**, 718 (2006).

[3] A. Simon, Phys. Rev. **98**, 317 (1955).

[4] F.F. Chen, *Intro. to Plasma Physics and Controlled Fusion,* Vol. 1, 2nd ed. (Plenum, New York, 1984), p. 239.

[5] A. Fruchtman, G. Makrinich, and J. Ashkenazy, Plasma Sources Sci. Technol. **14**, 152 (2005).

[6] D. Arnush, Phys. Plasmas **7**, 3042 (2000).

[7] F.F. Chen, Phys. Plasmas **19**, 093509 (2012).